PNAS
www.pnas.org

Supplementary Information for

Ultraviolet A light induces DNA damage and estrogen-DNA adducts in Fuchs endothelial corneal dystrophy: why females are more affected

Cailing Liu[a], Taiga Miyajima[a#], Geetha Melangath[a#], Takashi Miyai[a], Shivakumar Vasanth[a], Neha Deshpande[a], Varun Kumar[a], Stephan Ong Tone[a], Shan Zhu[a], Dijana Vojnovic[a], Yuming Chen[a], Eleanor G. Rogan[b], Muhammad Zahid[b], Ula V. Jurkunas[a*]

[*]Corresponding author**:** Ula V. Jurkunas, MD
E-mail: ula_jurkunas@meei.harvard.edu

This PDF file includes:

Supplementary text
Figures S1 to S5

www.pnas.org/cgi/doi/10.1073/pnas.1912546116

Supplementary Information Text

Materials and Methods

Experimental Animals

Ophthalmic examinations were performed one day prior and 1 day, 1 week, 2 weeks, 1, 2 and 3 months post UVA. Mouse estrous cycle was examined daily by visual vaginal observation at least 5 days before UVA irradiation. Female mice were irradiated at proestrus stage.

UVA lamp Assembly

We developed a customized experimental set up to irradiate the mouse eye in a controlled fashion with varying doses of UVA light. The assembly consists of a UVA LED light source (M365LP1, Thorlabs) producing 365 nm light and an LED driver (LEDD1B-T cube, Thorlabs) that modulates the current passing through it. Two lenses are employed in this set up. The beam of light from the source passes through the primary converging biconvex quartz lens (15 mm diameter and 8 mm focal length), placed close to the light source, which is further converged by the second fused quartz biconvex lens (1 inch diameter and 20 mm focal length) onto a 4 mm focal spot on the mouse cornea. All components are positioned collinearly on an aluminium base and fixed using supporting steel posts. The irradiation time (s) was calculated by multiplying the irradiance (W/cm^2) of the UVA source by the required irradiation dose (J/cm^2).

In vivo imaging

Anesthetized mice were restrained inside a DecapiCone holder during the imaging procedures.

In Vivo Confocal Microscopy

The mouse was wrapped with heat retention drapes (SpaceDrapes) on the platform that holds the mouse body securely for imaging CE cells by laser scanning IVCM using the Heidelberg Retina Tomograph III (HRT III) with Rostock Corneal Module (RCM) (Heidelberg Engineering, Germany). HRT III RCM is equipped with a 670-nm wavelength diode laser source and 63× objective immersion lens with a numerical aperture of 0.9 (Olympus, Tokyo). For each eye examination, a disposable sterile polymethylmethacrylate cap (Tomo-Cap; Heidelberg Engineering GmbH) filled with a drop of GenTeal gel eye ointment (hydroxypropyl methylcellulose 2.5% Novartis Ophthalmics, NJ) in the bottom was mounted in front of the cornea module optics. A drop of GenTeal gel was placed both on the eye and the tip of the objective lens to maintain immersion contact. During acquisition of images, the central cornea was made to focus on the instrument's red light fixation that was moved until the eye was in the imaging axis of RCM. The RCM objective lens was manually moved until the CE cells were in focus. The images were captured by scan mode of volume, sequence or

section. The laser confocal microscope acquires 2D-images that represent a coronal section of the cornea of 400 × 400 μm (160,000 μm^2) at a selectable corneal depth. Acquired images comprises 384 × 384 pixels and with a lateral resolution of 1 μm/pixel. Digital images were stored on a computer workstation at three frames per second.

Transmission electron microscopy

Mouse eyes were enucleated and immersion fixed with half strength Karnovsky's fixative (2% formaldehyde + 2.5% glutaraldehyde, in 0.1 M sodium cacodylate buffer, pH 7.4; Electron Microscopy Sciences, Hatfield, PA) at room temperature followed by dissecting the corneal cups. Corneal cups were placed back into the half strength Karnovsky's fixative for a minimum of 24 h under refrigeration. After fixation, samples were rinsed with 0.1 M sodium cacodylate buffer, post-fixed with 2% osmium tetroxide in 0.1 M sodium cacodylate buffer for 1.5 h, en bloc stained with 2% aqueous uranyl acetate for 30 min, then dehydrated with graded ethyl alcohol solutions, transitioned with propylene oxide and resin infiltrated in tEPON-812 epoxy resin (Tousimis, Rockville, MD) utilizing an automated EMS Lynx 2 EM tissue processor (Electron Microscopy Sciences, Hatfield, PA). Processed tissues were oriented in tEPON-812 epoxy resin and polymerized in silicone molds in an oven set at 60^{o}C. Semi-thin cross-sections for light microscopy were cut at 1 μm and stained with 1% toluidine blue in 1% sodium tetraborate aqueous solution for assessment and screening regions of the tissue block face for thin sectioning. Ultrathin sections (70-90 nm) were cut from the epoxy block using a Leica EM UC7 ultramicrotome (Leica Microsystems, Buffalo Grove, IL) and a diamond knife, collected onto 2x1mm single slot formvar/carbon coated grids and were stained with aqueous 25% Uranyl Acetate Replacement stain (Electron Microscopy Sciences, Hatfield, PA) and Sato's lead citrate using a modified Hiraoka grid staining system. Grids were imaged using a FEI Tecnai G2 Spirit transmission electron microscope (FEI, Hillsboro, OR) at 80 kV interfaced with an AMT XR41 digital CCD camera (Advanced Microscopy Techniques, Woburn, MA) for digital TIFF file image acquisition. TEM imaging of all layers of the cornea was assessed and images captured at representative regions.

Western Blotting

Mouse CE with DMs were dissected from corneal cup followed by lysis with the protein extraction buffer ER3 (Biorad; Hercules, CA) and 1 mM tributyl phosphine (TBP). Proteins were loaded onto 10% Bis-Tris NuPAGE gels (Thermo Fisher Scientific). Peptides were transferred to a polyvinylidene difluoride (PVDF) membrane (Millipore; Billerica, MA) and non-specific binding was blocked with 5% dry non-fat milk in PBS or 5% BSA in 0.05% Tween20/TBS for 1 h. Membranes were incubated overnight at 4˚C with anti-CYP1B1 (BD Biosciences #458511), anti-CYP1A1 (Abcam, #ab79819), anti-LC3 A/B (Cell Signaling, #3868), anti-COMT (Cell Signaling, #14368), and anti-NQO-1 (Abcam, #ab2346). anti-β-actin (Sigma-Aldrich, A1978) was used to normalize protein loading. Blots were rinsed, re-blocked, and exposed for 1 h to horseradish peroxidase (HRP)-

conjugated goat anti-rabbit IgG for CYP1B1, LC3A/B and COMT and HRP-conjugated donkey anti-mouse IgG for β-actin blots. After washing in 0.05% Tween20/PBS, antibody binding was detected with a chemiluminescent substrate (Thermo Scientific). Densitometry was analyzed with ImageJ software (NIH), and protein content was normalized relative to β-actin.

Mitochondrial fractionation

For assessing the mitochondrial levels of CYP1B1 in UVA treated HCEnC-21T cells, mitochondria were purified using BioVision Mitochondria/Cytosol Fractionation Kit (Cat no-K256-25) according to manufacturer's instructions. The fractions were loaded onto 10% Bis-Tris NuPAGE gels for western blotting as described above. Rabbit polyclonal anti-CYP1B1 (Abcam, # ab185954), VDAC (Abcam, # ab18988) and GAPDH (Sigma, G9545) primary antibodies were used.

Statistical Analysis

Results were expressed as the mean ± SE. Data of cell density, hexagonality, coefficient of variation, ROS production, TUNEL labeled apoptotic cells and CYP1B1 levels were analyzed using a two-tailed unpaired Student's *t*-test. Longitudinal CCT data were analyzed by mixed effect regression analysis (Stata 14, StataCorp LLC, TX). LA-qPCR results were analyzed by two-way analysis of variance with Bonferroni post hoc test (Graphpad Prism 5, Graphpad Software Inc, CA). $P < 0.05$ was considered statistically significant.

Figure S1

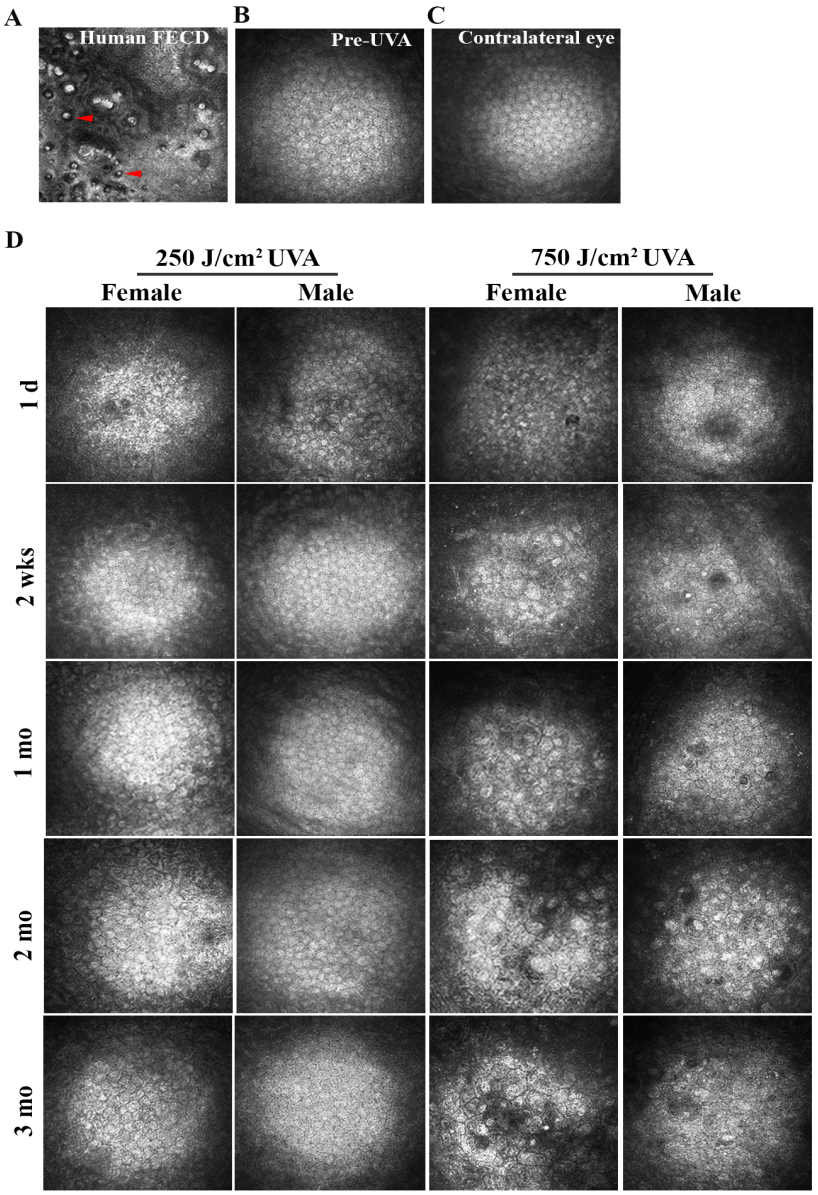
A
Human FECD
B
Pre-UVA
C
Contralateral eye
D
250 J/cm² UVA
750 J/cm² UVA
Female
Male
Female
Male
1 d
2 wks
1 mo
2 mo
3 mo
E
1 mo post UVA
Female
Male
cells/mm²
3000
2500
2000
1500
1000
500
0
*
*
0
250
500
750
1000
J/cm²

Fig S1. In vivo confocal HRT photographs of CE from FECD patient (*A*). Red arrowheads indicate guttae. MCEnCs before UVA treatment (*B*) and from the contralateral eye (*C*) without UVA. (*D*) Confocal HRT photographs of female or male MCEnC with treatment of 250 and 750 J/cm^2 UVA at 1 day, 2 weeks, 1, 2 and 3 months post UVA (*E*) Corneal endothelial cell density analysis of female (white) and male (black) mice at 1 month post various doses of UVA. * $p < 0.05$

Figure S2

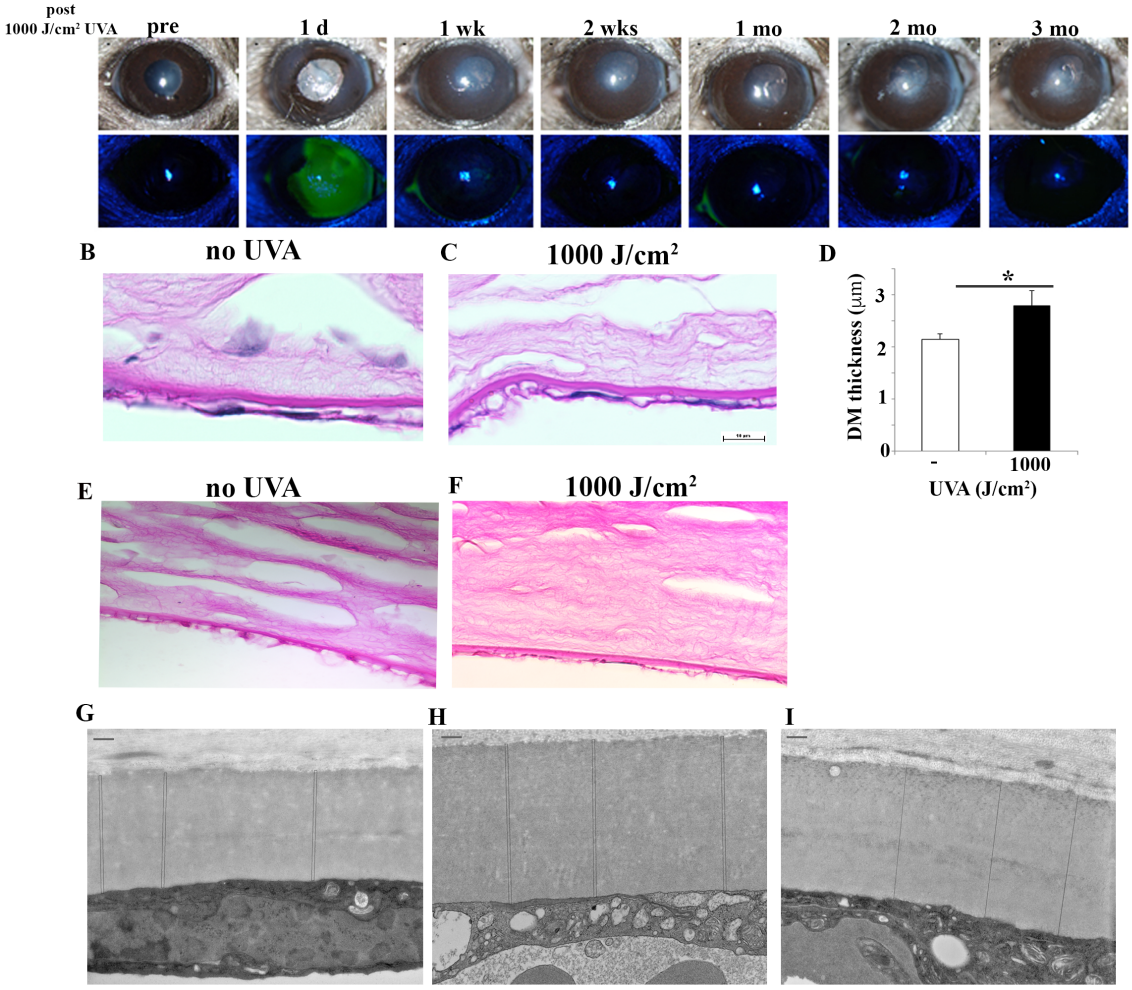

Fig S2. (*A*) Representative *in vivo* slit lamp images showing mouse corneal clarity (upper row) and fluorescein staining of the corneal epithelial surface (lower row) before UVA and at 1 day, 1 week, 2 weeks, 1, 2 and 3 months post 1000 J/cm^2 UVA. (*B*) Representative phase contrast microcopy images of mouse corneas stained with P&S (**B&C**) showing DM thickness in 1000 J/cm^2 UVA-irradiated mouse corneas and controls (60x) (*D*, data generated from 2 females and 1 male). (*E, F*) Lower magnification images of P&S staining of 1000 J/cm^2 UVA-irradiated mouse corneas and controls (40x). (*G*) Representative TEM images of DM of mouse corneas without UVA (*F*, female, x 18500**)** and with 1000 J/cm^2 UVA (*H*, female; *I*, male; x18500).

Figure S3

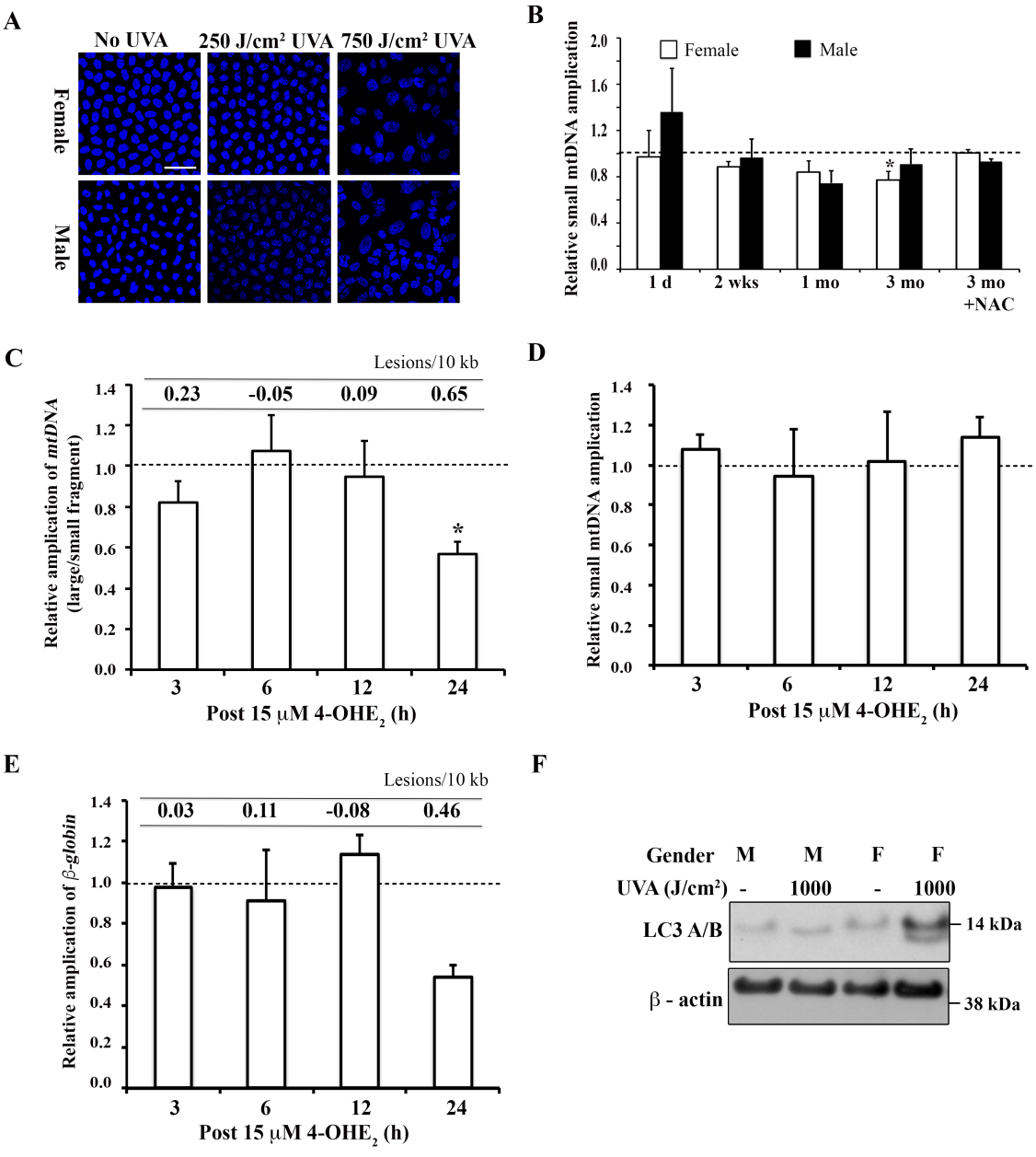

Fig S3. (*A*) Representative confocal images of whole mount of female (upper panels) and male (lower panels) mouse CE with labeling of TUNEL (pink) 3 months post 250 or 750 J/cm^2 UVA. DAPI was used for nuclei staining (blue). (*B*) Detection of MCEnC mitochondrial copy number at various time points post 1000

J/cm^2 UVA irradiation. LA-qPCR analysis of mtDNA damage (*C*) and mtDNA copy number (*D*) in HCEnC-21T cells treated with 4-OHE_2 for varying time points. (*E*) Analysis of DNA lesion frequency in the nDNA encoded ß-globin gene in HCEnC-21T cells treated with 4-OHE_2 treatment. Data are mean ± SEM, $*P < 0.05$ by two-way ANOVA (*F*) Western Blot of LC3 A/B levels in male and female MCEnCs 1 day post 1000 J/cm^2 UVA irradiation.

Figure S4

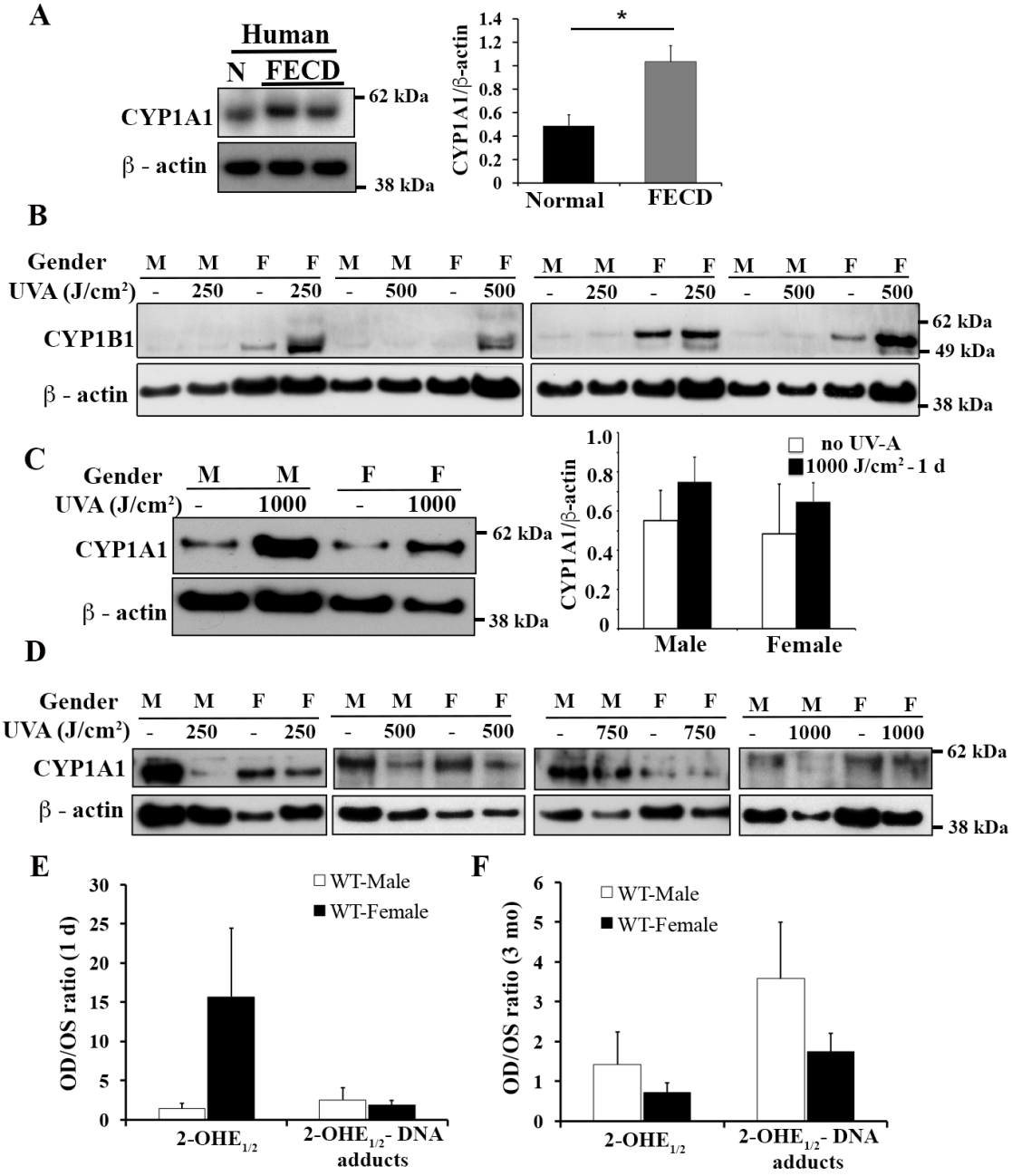

Fig S4. (*A*) Western blotting of CYP1A1 levels in both sexes in normal (n=5) and FECD (n =14) *ex vivo* specimens. β-actin is used as normalizing control. Densitometric analysis of the protein levels is represented as bar graph; black and grey bars denote normal and FECD, respectively. ***$P < 0.001$ by two tailed Students *t* test. (*B*) Western blotting of CYP1B1 in both male and female MCEnCs at 3 months post various fluences of UVA irradiation. (*C*) Western blotting of CYP1A1 levels in male and female MCEnCs 1 day post 1000 J/cm^2 UVA. Corresponding densitometric analysis is represented as bar graph to the right. White and black bars denote no UVA and 1000 J/cm^2 UVA, respectively.

(*D*) CYP1A1 levels in male and female MCEnCs after 3 months post UVA irradiation with 250, 500, 750 and 1000 J/cm^2 doses by western blotting. (*E, F*) Ratio of OD (treated) by OS (untreated) of 2-OHE$_{1/2}$ generated by CYP1A1 and corresponding 2-DNA adducts in male and female MCEnCs 1 day (*E*) and 3 months (*F*) post 1000 J/cm^2 UVA.

Figure S5

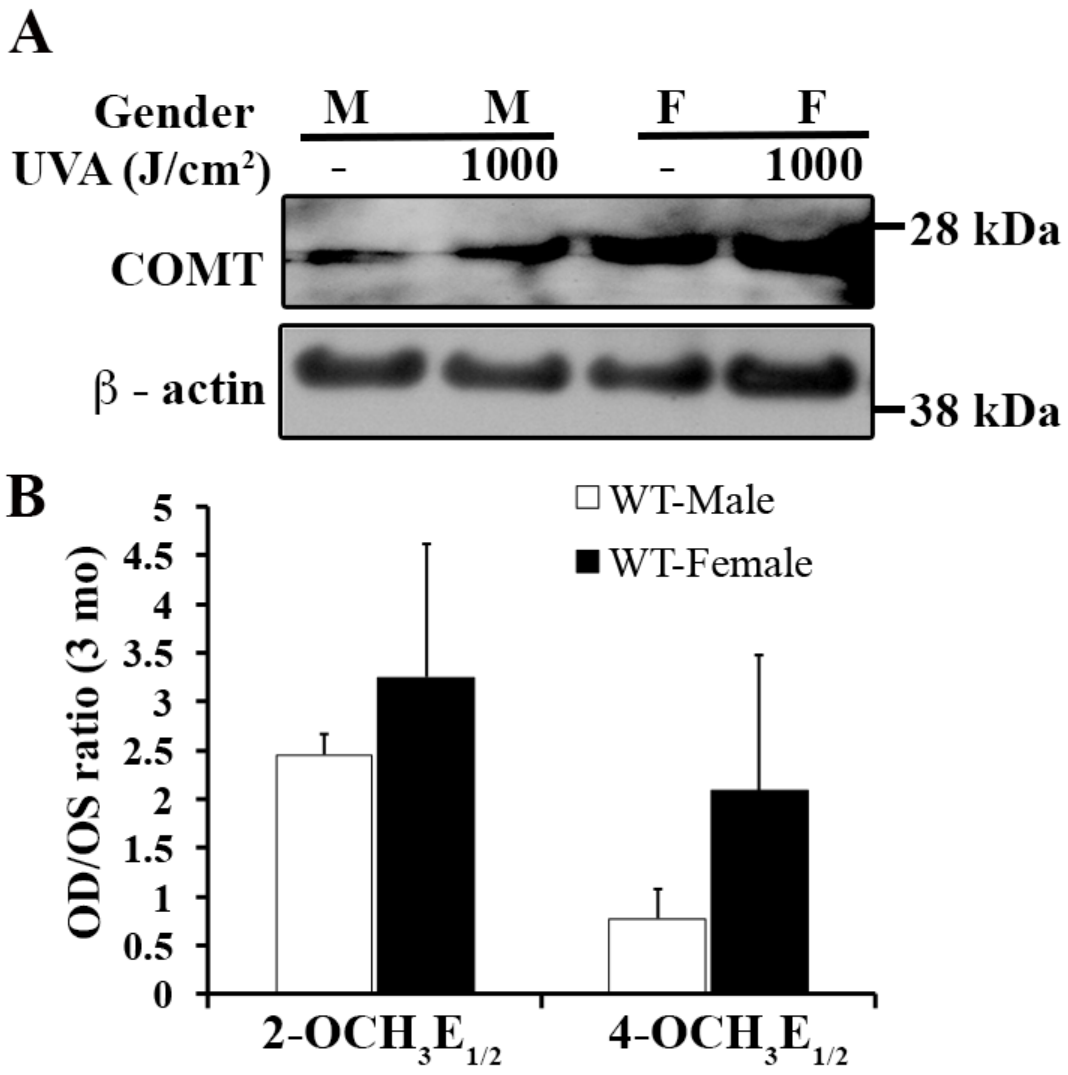

Fig S5. (*A*) Western blot of COMT levels in male and female MCEnCs 1 day post 1000 J/cm^2 UVA. β-actin served as normalizing control. (*B*) OD/OS ratio of levels of 4-OCH3E$_{1/2}$ and 2-OCH3E$_{1/2}$ metabolites generated by COMT in male and female MCEnCs 3 months post 1000 J/cm^2 UVA.